ARTICLES

Direct Observation of the Thermal Decomposition of Ligand-Stabilized Clusters

G. Radu, U. Memmert,† H. Zhang, G. Nicolay, F. Reinert, and U. Hartmann*

Institute of Experimental Physics, University of Saarbrücken, P.O. Box 151150, D-66041 Saarbrücken, Germany

Received: September 5, 2001; In Final Form: July 2, 2002

Ligand-stabilized Au_{55} clusters have been observed by scanning probe microscopy upon thermal decomposition on top of graphite and mica substrates. On highly oriented pyrolitic graphite as well as on mica the ligand shell exhibits a thermal decomposition at a temperature of about 390 K. This temperature well matches data obtained on cluster solutions and pallets. The ligand decomposition results under ultrahigh vacuum conditions in the formation of naked Au clusters. The in situ needle sensor studies show that, due to the high cluster mobility at elevated temperatures, bigger spherical Au aggregates are formed on the graphite substrate. In contrast, on the mica substrate, the naked Au clusters aggregate to form small uniform islands that are stable up to temperatures of more than 700 K. Bigger Au aggregates could only be formed upon pushing the clusters by the microscope's probe at elevated temperatures. The significant difference in the cluster decomposition and aggregation processes on graphite and mica is attributed to the influence of a strong cluster−substrate interaction, which is solely present for mica.

1. Introduction

Clusters consisting of a few up to a few hundreds of atoms are of fundamental as well as of applied interest because they exhibit interesting size-effect-dominated physical and chemical properties.[1−3] In particular, ligand-stabilized clusters are chemically largely inert and thus allow investigations under ambient conditions,[4,5] whereas naked clusters can in general only be studied under ultrahigh vacuum (UHV)[6] or electrochemical conditions.[7] On the other hand, it is evident that ligand-stabilized clusters do generally not exhibit the properties of the naked cluster core but involve a more or less significantly pronounced influence of the ligand shell on their overall physical and chemical properties. An additional aspect is that, upon investigating the properties of ligand-stabilized clusters on top of solid substrates, the influences of cluster−cluster as well as cluster−substrate interactions generally have to be taken into account.[8]

One of the most intensely studied ligand-stabilized clusters is Au_{55}, first synthesized by Schmid's group.[9] Due to the sufficiently small number of Au atoms the clusters exhibit strongly size-effect-dominated physical properties.[4,5] Thus, Au_{55} is particularly interesting for fundamental investigations, e.g., on quantum electronic phenomena. It has even been emphasized that it might even be possible to base applications in terms of quantum devices on the employment of individual Au_{55} clusters.[10]

One aspect of importance with respect to any research or application concept is the structural stability of the clusters and, in particular, the stability upon heating. So far, heating experiments have rigorously only been performed on solutions and bulk samples using standard methods of calorimetry.[11] In the present work we report on direct observations of the thermal decomposition of Au_{55} clusters on top of highly oriented pyrolitic graphite (HOPG) and mica substrates under UHV conditions. The clusters have been deposited as disordered monolayers. The observations have been performed in situ using needle-sensor microscopy (NSM) and have been extended by ex situ observations using scanning electron microscopy (SEM). For comparison, additional heating experiments on the ligand molecules adsorbed to a (111)-oriented Au thin film were performed.

2. Sample Preparation and Experimental Setup

Ligand-stabilized Au_{55} clusters, such as $Au_{55}(PPh_3)_{12}Cl_6$ were produced by a wet-chemical process as described elsewhere.[9] The clusters contain a metallic core of 1.4 nm diameter composed of 55 Au atoms in a two-shell closed-packed arrangement with the outer atoms stabilized by an organic ligand shell that can be "designed" to be of a well-defined thickness.[12] The size of the $Au_{55}(PPh_3)_{12}Cl_6$ cluster including its ligand shell is approximately 2.1 nm. Mica and HOPG were cleaved using the adhesive-tape method and employed as substrates for cluster deposition. The clusters were dissolved in dichlormethane (CH_2Cl_2) and deposited onto freshly prepared substrates by spin coating.

Variable-temperature experiments were performed in UHV with a commercial scanning probe microscope[13] in the needle-sensor mode[14] on clusters on top of both substrates. The samples were transferred into the UHV chamber via a fast sample load lock immediately after ex situ preparation. They were investigated at varying temperatures in the range between 300 and 750 K.

* Corresponding author. E-mail: u.hartmann@mx.uni-saarland.de.
† Present address: Atotech Deutschland GmbH, P.O. Box 210780, 10507 Berlin.

10.1021/jp013409z CCC: $22.00
Published on Web 09/17/2002

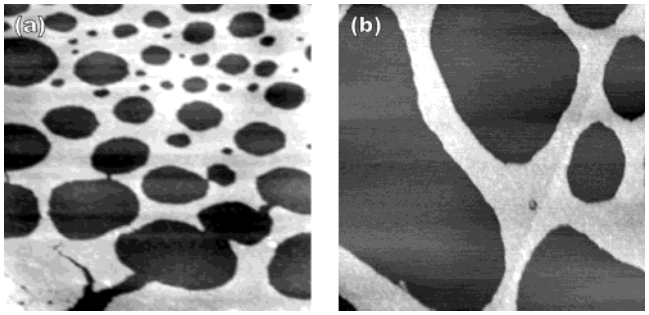

Figure 1. NSM images of disordered Au_{55} monolayers deposited by spin coating on mica (a) and HOPG (b). The scanned area is 1 μm × 1 μm, respectively.

SEM[15] investigations were performed on Au_{55} layers on HOPG for as-deposited samples and for samples previously annealed for 2 h in UHV at several predetermined temperature values. The procedure involves, for a given sample, repeated cycles of imaging and annealing at successively increasing temperature.

Using UHV-variable-temperature STM[16] imaging of the ligand molecules (PPh_3) deposited on top of an Au(111) thin film was performed for as-deposited samples as well as for samples previously heated to a certain temperature. The PPh_3 molecules in crystalline arrangement were dissolved in CH_2Cl_2 and deposited by spin coating on the gold substrate which was prepared according to ref 16.

The experiments were completed by X-ray photoelectron spectroscopy (XPS) on Au_{55} layers deposited on HOPG by spin coating. Spectra were taken from as-deposited samples and samples previously heated to various temperatures.

3. Experimental Results

For a highly diluted cluster solution one typically observes disordered cluster monolayers with pores of varying size. In the latter the bare substrate is exposed. However, upon comparing the detailed layer topology, it turns out that for HOPG the size distribution and density of the pores exhibits a stronger variation than for mica. Images were taken at various locations on one given sample. The uncovered areas vary between 47% and 57% for mica and 58% and 70% for HOPG. Wetting of HOPG by the cluster solution appears to be worse compared to mica. The overall appearance of the cluster layers is the same on both substrate types.

Figure 1 shows typical NSM images of Au_{55} monolayers on HOPG and mica substrates. The arrangement of the pores within the disordered layers is evident. The samples could be imaged without any noticeable perturbation by the needle sensor probe.

The clusters on mica can be imaged as in Figure 1a up to a temperature of about 390 K without any obvious change in the layer structure. Then, upon exceeding this temperature, imaging conditions become suddenly unstable and no data acquisition is possible anymore. Subsequently, after a further temperature increase, stable imaging again becomes possible. The layer exhibits a certain increase in the overall roughness at unchanged overall topology. The maximum corrugation is obtained at a temperature of about 530 K. Above this value the roughness stays constant. Figure 2 shows a comparison between the fairly smooth layer at 340 K and almost the same surface area at 540 K and respectively increased corrugation.

The layer morphology displayed in Figure 2b appears to be stable up to a temperature of at least 750 K, which was the maximum accessible value. The granularity could only be significantly modified upon repeated scanning at elevated

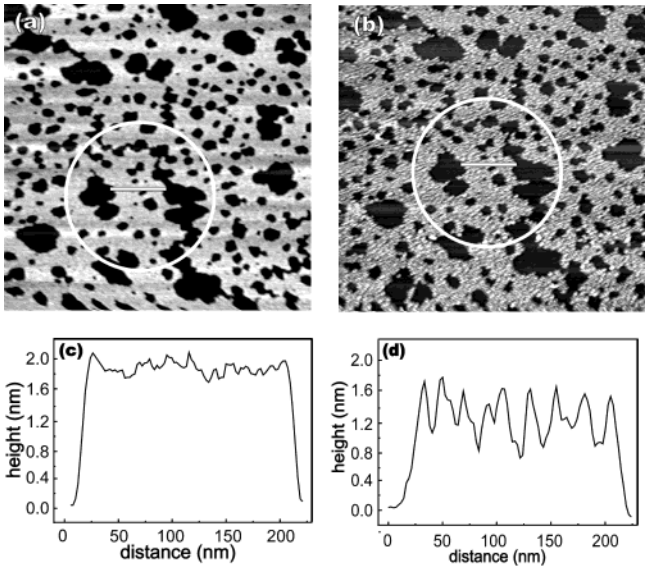

Figure 2. NSM images prior (a) and subsequent to (b) the thermally induced decomposition of Au_{55} on mica. The images of size 1.2 μm × 1.2 μm were taken at 340 and 540 K and exhibit almost the same area. The encircled regions precisely correspond to each other. The indicated line scans are displayed in (c) and (d). They clearly show an increase in surface roughness at decreased layer thickness after passing through the decomposition temperature.

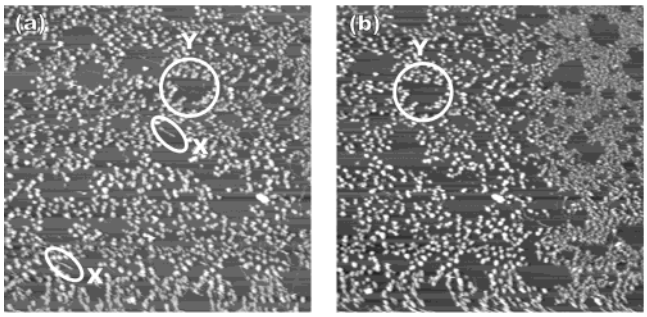

Figure 3. 1.2 μm × 1.2 μm NSM images of a cluster layer on mica taken at 570 K. After the same frame is scanned six times, considerable tip-induced aggregation is obvious in (a). At the encircled positions marked by "x" tip-induced particle motion is directly visible. After another three frames are scanned (b), tip-induced aggregation has proceeded. The encircled area marked by "y" is precisely the same in both images. The right part of (b) shows an area of the cluster film that has not been scanned before. The less pronounced aggregation is obvious.

temperature. Obviously, the interaction of the layer with the needle probe causes enough mobility of the grains or islands in the layer to form bigger aggregates. Figure 3 shows two images of almost the same surface area, where three frames have been taken in between. Additionally Figure 3b shows at the right-hand side a virginal part of the layer that has not been imaged before. In Figure 3a two locations are marked, where imaging is dominated by destructive tip−layer interactions stimulating aggregation. In Figure 3b the significantly different extent of aggregation of the frequently scanned part of the image and the virginal one is obvious. Imaging the samples at room temperature after cooling from any temperature above 390 K does not change the extent of aggregation in contrast to scanning at elevated temperature.

On HOPG the cluster decomposition and aggregation process turns out to be significantly different from that on mica. First of all, NSM imaging of the clusters is, due to a high cluster mobility even at room temperature, more delicate than on mica.

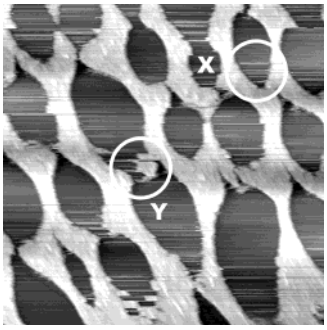

Figure 4. 1.2 μm × 1.2 μm NSM image of a cluster layer deposited on HOPG taken at 400 K. Much stronger probe-induced perturbations than for mica are clearly obvious. In the encircled areas small ("x") and extended ("y") areas of shifted material are indicated.

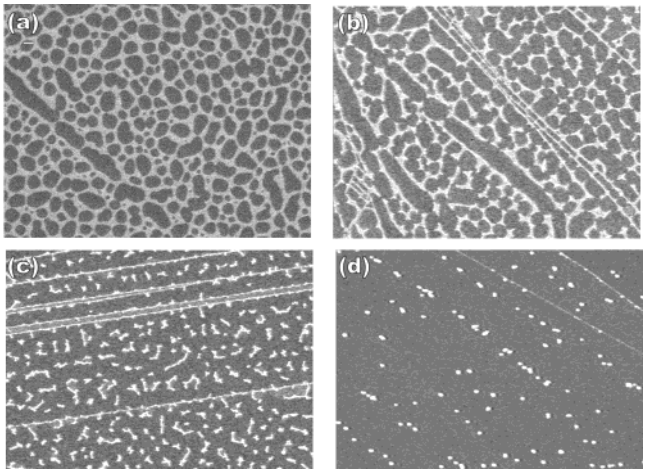

Figure 5. Ex situ 5.6 μm × 4.2 μm SEM images of cluster layers on HOPG as deposited (a) and after 2 h of annealing in UHV at 400 K (b), 420 K (c), and 520 K (d), respectively.

The imaging instability, obviously related to the first cluster decomposition step appears at almost the same temperature as observed on mica. When the decomposition temperature is exceeded, NSM imaging at a given temperature involves much more perturbation due to probe−cluster interactions than on mica. Figure 4 shows various distinct small and also extended probe-induced shifts of material observed at about 400 K. The latter value is clearly above the decomposition temperature.

Due to the problems in imaging the HOPG-based sample by NSM, the aggregation behavior at elevated temperatures was studied in terms of ex situ SEM observations following the experimental procedure mentioned before. Figure 5 shows a series of images taken for one sample in the temperature range between room temperature and about 520 K. The instability observed in the NSM images occurs between those temperatures at which parts a and b of Figure 5 were taken. The significant structural change related to the instability is clearly obvious. A certain aggregation of material has taken place, and the step edges of the substrate became decorated. Upon a further increase in the annealing temperature, the aggregation proceeds until only individual dots remain. Due to the missing three-dimensional resolution of SEM, it is not obvious that the dots are largely spherical. This became clear from additional NSM line profiles.

To investigate the behavior of the ligand molecules independently from the clusters, ligand-covered Au thin films were investigated for comparison. After the deposition on the gold substrate, the ligand molecules (PPh_3) form a disordered monolayer on the surface. The sample was first heated to 390 K for 2 h and to 470 K for 15 min and imaged by STM after

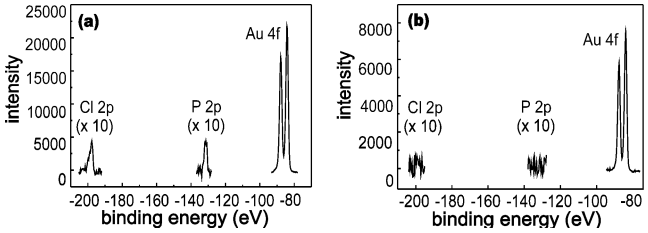

Figure 6. XPS spectra of Au_{55} layers deposited on HOPG after sample preparation (a) and after heating to 565 K for 2 h (b).

cooling to room temperature for each heating cycle. The STM images show that after heating to 390 K, the molecules form aggregates of various sizes between two and several tens of molecules. Further heating to 470 K causes the molecules to completely disappear from the substrate.

Information about the stability of the cluster compound during heat treatment can ultimately only be obtained from the XPS measurements. Figure 6 shows the spectra for an as-deposited sample and a sample heated for 2 h to 565 K. The stoichiometry with respect to the Cl, P, and Au atoms is perfectly represented by the spectrum in Figure 6a. The heating procedure, however, completely removes the Cl and P peaks from the data, as becomes obvious in Figure 6b. It can thus be concluded that the ligand shell completely desorbs.

4. Discussion and Interpretation

Ligand-stabilized Au_{55} clusters are chemically largely inert.[5] This implies that the clusters can interact with each other or with a substrate only via van der Waals, steric, and Coulomb interactions. The behavior of the clusters for the as-deposited samples is slightly different for HOPG and mica. This is due to the totally different surface properties of the two substrates: the HOPG cleavage plane is uncharged and chemically inert, whereas the mica surface involves charges. In muscovite-type mica, $KAl_2(AlSi_3O_{10})(OH)_2$, every fourth Si is substituted by Al in the tetrahedral sheet. This produces a charge of -1 per formula unit. The additional charge is satisfied by K^+ ions that reside in the interlayer cavities bound such that it is not exchangeable.[17] The actual charge distribution at and in the vicinity of the mica surface appears to be quite complicated and depends on the cleavage conditions.[18] Cleavage occurs along the (001) plane involving a hexagonal array of K^+ ions. It is believed that upon cleavage the K^+ ions are distributed equally between the newly created surfaces. Clean surfaces exhibit a significant variation of the surface charge density from region to region at a macroscopic scale, where positive as well as negative charging can occur.[18,19] Exposure to atmospheric contaminants considerably reduces the measurable surface charge.[18] Furthermore, the mica surface is known to be chemically reactive, which is of predominant relevance to certain adhesion and bonding phenomena.[18]

The different wetting behavior of the dichloromethane-based cluster solution and the resulting formation of the disordered monolayers on both substrates is a consequence of an interplay between clusters, solvent, and substrate upon evaporation of the solvent. The surface charge of the mica substrate is of importance for that interplay. As mentioned before, wetting is worse for the HOPG substrate. Furthermore, NSM imaging on the as-deposited samples confirms that the cluster mobility during the imaging process is clearly higher for HOPG, making this sample more sensitive to probe-induced perturbations. Thus, in conclusion, all the above observations support that mica attracts ligand-stabilized Au_{55} stronger than HOPG due to its surface charge density.

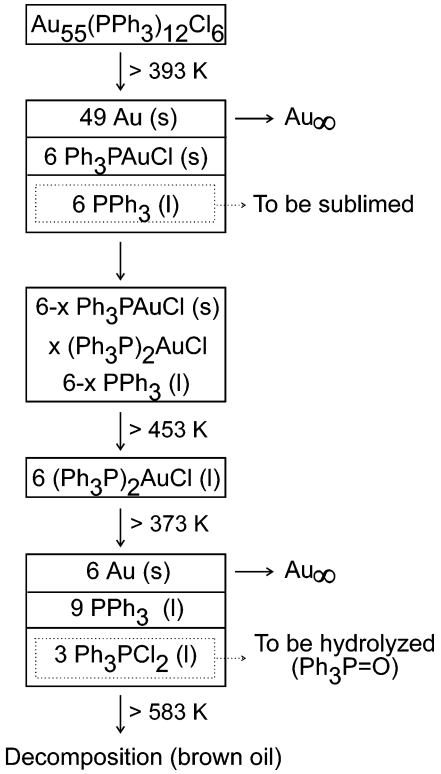

Figure 7. Hypothetical Au_{55} decomposition scheme partly supported by impedance and DSC measurements on bulk Au_{55} pallets and solutions.[11]

Differential scanning calorimetry (DSC) measurements on cluster solutions revealed an exothermic decomposition in the temperature range between 404[11] and 429 K.[20] These observations as well as impedance measurements on cluster pallets[21] and further investigations led to the cluster decomposition scheme shown in Figure 7. On both substrates we observed in the NSM images an instability at a temperature of about 390 K, where imaging turned out to be impossible. Below and above this temperature no such unstable imaging conditions were observed. A temperature of 390 K agrees fairly well with the onset temperature observed in the DSC measurements.[11] In this context it is worth mentioning that in our NSM experiments, the temperature control was not very precise. Starting with the onset, however, the decomposition and aggregation processes proceed quite differently for mica and HOPG.

An essential question is, does heating of the ligand-stabilized clusters really lead to a complete desorption of the ligand molecules or does some residual of the ligand shell remain? Heating of the ligand-coated Au thin films and subsequent high-resolution STM analysis show that at least on the extended Au substrate no residuals remain. Clarity is provided by the XPS data taken on Au_{55} layers deposited on HOPG (see Figure 6). Heating the sample to well above the decomposition temperature of 390 K completely removes all residuals of the ligand shell.

For mica the local pattern consisting of pores and extended areas of the disordered cluster monolayer is largely conserved upon passing the first decomposition step. Obviously, the ligands desorb in the absence of a spontaneous and pronounced aggregation of the naked Au clusters (see Figure 2). The thickness of the Au_{55} monolayer prior to decomposition (Figure 2c) coincides fairly well with what is usually measured for an individual ligand-stabilized cluster.[22] The layer thickness decreases by about 3−4 Å after desorption of the ligands, which is in accordance with what is expected for the naked cluster.[1] The overall conservation of the layer topology and in particular the fact that the layer thickness remains comparable with the diameter of a naked cluster again confirms the existence of a relatively strong cluster−substrate interaction.

The surface charge of mica, which may involve a complex large-scale patch charge distribution,[18,19] gives rise to electrostatic interactions with the clusters. Au_{55} somehow behaves like bulk Au, which is electronegative.[23] It is furthermore instructive to compare the observations with results from Au/mica adhesion experiments.[18] For clean surfaces, i.e., under permanent UHV conditions, Au films make intimate contact with the mica surface and the sites for the stronger adhesion of Au adatoms are those situated between the K^+ ions, i.e., oxygen sites and vacant K^+ sites. A priori van der Waals interactions, chemical interactions, and electrostatic forces need be considered for the adhesion of Au to mica. In this case chemical interactions include covalent, ionic, and metallic bonding. Electrostatic forces include image forces and Coulomb forces due to contact charging. The latter results from electron transfer across the metal/dielectric interface due to work function differences. For the adhesion of Au to UHV-cleaved mica a comparison of the possible interaction mechanisms led to the conclusion that a substantial chemical contribution is likely to be involved in the bonding across the interface.[18] In contrast, the adhesion of Au to air-cleaved mica is more consistent with the predominance of van der Waals forces.[18] In this case the reactive sites are occupied by carbon or hydrocarbons and thus do not contribute to metal atom adhesion. Because in the present experiments cleavage had to be performed ex situ, we have to assume that our substrates are contaminated. That implies that the reactive sites are largely saturated, van der Waals interactions are partly screened, and free charges are considerably lowered. Nevertheless, intimate contact between adherents and substrate could occur at certain randomly distributed sites. Bonding to the mica substrate drastically restricts the mobility of the naked Au clusters, which are generated according to the scheme in Figure 7 or at least in a similar way. Instead of extended Au islands or grains, only moderate aggregation of the naked clusters takes place upon temperature increase. Parts a and d of Figure 2 show that the aggregates exhibit a diameter of a few nanometers. The thickness remains independent of the temperature and approximately corresponds to the diameter of a naked cluster core. The overall topology is conserved up to temperatures of at least 750 K at only slightly increasing surface corrugation (see Figure 2). Bonding to the mica surface clearly keeps the naked clusters from forming extended Au aggregates. Extended aggregation can only be initiated if the separated small aggregates are pushed together by the NSM probe at elevated temperatures. In this case bigger Au grains can be generated (Figure 3).

On HOPG such Au grains result from an unrestricted aggregation of the naked clusters upon temperature increase. Due to the absence of a pronounced cluster−substrate interaction, the high cluster mobility leads after decomposition of the ligands to an immediate aggregation, which at the initial step still reflects the overall structure of the disordered monolayer (Figure 4). Upon a further increase in temperature, the monolayer step edges of the HOPG substrate are decorated by Au due to their heigher chemical reactivity (Figure 5b−d). Ultimately, the proceeding aggregation process leads to individual Au islands or grains of slightly varying size that are clearly separated and are partly aligned along the step edges (Figure 5d). The fundamental difference in the cluster decomposition and aggregation processes on the two substrates becomes obvious from a direct comparison of Figure 2b,d).

5. Conclusions

In conclusion it has been observed by in situ NSM and ex situ SEM experiments that the thermally induced decomposition of $Au_{55}(PPh_3)_{12}Cl_6$ and subsequent aggregation of the residuals, i.e., pure Au, takes place in a very different way on mica and HOPG substrates. This is attributed to a stronger interaction between Au_{55} and mica on one hand and between Au_∞ and mica on the other hand. Because the ex situ cleaved substrates are contaminated, it is assumed that the major contributions to the interaction with mica are electrostatic and van der Waals forces rather than chemical bonds. The relative contribution of the different interactions, however, could not be deduced. The cluster−substrate interaction conserves the overall monolayer topology even after thermally decomposing the cluster ligands. The onset of thermal decomposition coincides with that observed in DSC and impedance measurements. The complete desorption of the ligand molecules is observed directly for layers on Au(111)-oriented thin films by STM. Furthermore, XPS data confirm that no residuals of the ligand shell remain after heating Au_{55} layers on HOPG to above the decomposition temperature. On HOPG the cluster−substrate interaction is much weaker and electrostatic forces and chemical interactions can be excluded. As a consequence, the clusters are highly mobile. The Au residuals after thermal decomposition, which takes place at about the same temperature as for mica, rapidly aggregate upon increasing the temperature.

Acknowledgment. We not only acknowledge the kind supply of the Au_{55} clusters by G. Schmid from the University of Essen but also very helpful and clarifying discussions with him.

References and Notes

(1) Schmid, G. *Clusters and Colloids − From Theory to Applications*; Schmid, G., Ed.; VCH: Weinheim, 1994; Chapter 3.
(2) Haberland, H. *Clusters of Atoms & Molecules − Theory, Experiment, & Clusters of Atoms*; Haberland, H., Ed.; Chemical Physics Series, Vol. 52; Springer: New York, 1994.
(3) Kreibig, U.; Vollmer M. *Optical Properties of Metal Clusters*; Springer: Berlin, 1995.
(4) Schmid, G. *Chem. Rev.* **1992**, *92*, 1709.
(5) Schmid, G.; Chi, L. F. *Adv. Mater.* **1998**, *10*, 515.
(6) Ganz, E.; Sattler, K.; Clarke, J. *Surf. Sci.* **1989**, *219*, 33.
(7) Kolb, D. M.; Ullmann, R.; Ziegler, J. C. *Electrochim. Acta* **1998**, *43*, 2751.
(8) Feigenspan, Th.; Houbertz, R.; Hartmann, U. *NanoStruct. Mater.* **1997**, *9*, 367.
(9) Schmid, G.; Pfeil, R.; Boese, R.; Bandermann, F.; Meyer, S.; Calis, G. H. M.; van der Velden, J. A. M. *Chem. Ber.* **1981**, *114*, 3634.
(10) Simon, U. *Adv. Mater.* **1998**, *10*, 1487.
(11) Schmid, G.; Hess, H. **1995**, *621*, 1147.
(12) Schmid, G. *Chem. Rev.* **1992**, *92*, 1709.
(13) UHV VT-SPM, Omicron Instruments.
(14) Bertzke, K.; Antrack, T.; Schmidt, K.-H.; Dammann, E.; Schatterny, Ch. *Int. J. Optoelectron.* **1993**, *8*, 669.
(15) Field emission SEM Hitachi S-4500.
(16) Zhang, H.; Memmert, U.; Houbertz, R.; Hartmann, U. *Rev. Sci. Instrum.* **2001**, *72*, 2613.
(17) Sharp, G. T.; Oden, I. P.; Buseck, R. P. *Surf. Sci. Lett.* **1993**, *284*, 405.
(18) Higginbotham, I. G.; Williams, R. H.; McEvoy, A. J. *J. Phys. D: Appl. Phys.* **1975**, *8*, 1033.
(19) Metsik, M. S.; Golud, L. M. *Sov. Phys. − Dokl.* **1972**, *17*, 472.
(20) Benfield, R. E.; Creighton, J. A.; Eadon, D. G.; Schmid, G. *Z. Phys. D* **1989**, *12*, 533.
(21) Simon, U.; Schön, G.; Schmid, G. *Angew. Chem.* **1993**, *105*, 264.
(22) Houbertz, R.; Feigenspan, T.; Mielke, F.; Memmert, U.; Hartmann, U.; Simon, U.; Schön, G.; Schmid, G. *Europhys. Lett.* **1994**, *28*, 641.
(23) Schmid, G. *Endeavour New Series* **1990**, *14*, 172.